Ecological Modelling 428 (2020) 109055

Contents lists available at ScienceDirect

Ecological Modelling

journal homepage: www.elsevier.com/locate/ecolmodel

The energetic basis of population growth in animal kingdom

Sebastiaan A.L.M. Kooijman[*,a], Konstadia Lika[b,c], Starrlight Augustine[d], Nina Marn[e,f], Bob W. Kooi[a]

[a] Department of Theoretical Biology, VU University Amsterdam, de Boelelaan 1087, 1081 HV Amsterdam, the Netherlands
[b] Department of Biology, University of Crete, 70013, Heraklion, Greece
[c] Institute of Computational Mathematics, Foundation of Research and Technology Hellas, 70013 Heraklion, Greece
[d] Akvaplan-niva, Fram High North Research Centre for Climate and the Environment, 9296 Tromsø, Norway
[e] Division for Marine and Environmental Research, Rudjer Boskovic Institute, 10 000 Zagreb, Croatia
[f] School of Biological Sciences - Faculty of Science, University of Western Australia, Perth WA 6009, Australia

ARTICLE INFO

Keywords:
Dynamic energy budget theory
Add-my-Pet
Characteristic equation
Specific population growth rate
Thinning
Macro-chemical reaction equation
Co-variation of parameters
Body size scaling
Metabolic acceleration
Specific growth rate of structure
Waste-to-hurry
Supply-demand spectrum
Altricial-precocial spectrum
Evolutionary relict

ABSTRACT

Population growth, and other population characteristics, have been computed and made available online for over 2000 animal species in the Add-my-Pet (AmP) collection, assuming constant food and temperature environments. The AmP collection – online database of Dynamic Energy Budget model parameters, implied properties and referenced underlying data – provides an unique opportunity to study how energetics of individuals relates to population growth. For the comparisons of traits, we assume that the background hazard rate is zero, but aging applies to all species and 'thinning' to species with high reproduction rates. The new concept 'thinning' is a state-dependent hazard rate such that the feeding rate of a cohort does not change in time: the increase of individual feeding rates due to growth is exactly compensated by a reduction in numbers. Thinning affects population growth rate, but the impact differs substantially between species. Some 11% of species do not survive thinning, even at abundant food. The population growth rate relates to the underlying energetics; we discuss and suggest explanations for how population growth rates fit into all known patterns in the co-variation of parameter values: body size-scaling, metabolic acceleration, waste-to-hurry, supply-demand spectrum and altricial-precocial spectrum. We show that, after reproduction, age at puberty dominates population growth. The specific population growth rate scales with maximum body weight in the same way as the weight-specific respiration scales with body weight. DEB theory, which explains both, shows, however, that no direct relationship exists between the population growth rate and respiration. We suggest that the similarity in scaling results from the equality between specific population growth and specific growth rate at maximum growth of structure, and might be an evolutionary relict from times that life consisted of dividing unicellulars; population and body growth are directly connected for unicellulars. We show that the specific growth rate at maximum growth equals 1.5 times the von Bertalanffy growth rate, in a DEB context, which is a new interpretation of the latter growth rate. We expected the population growth rate to co-vary with specific somatic maintenance rate, based on a previously discovered pattern, called the waste-to-hurry strategy, where growth and reproduction are increased by simultaneously increasing assimilation and somatic maintenance in species that live off temporarily abundant food supplies. We did find this effect in ecdysozoa and spiralia, which comprise roughly 95% of animal species, but hardly so in tetrapods. The reason might be that specific somatic maintenance also co-varies with specific maturity levels at puberty for tetrapods. The scaled functional response at which the population growth rate is zero is very close to that at which puberty can just be reached in absence of thinning, and somewhat higher in presence of thinning. The specific population growth rate at abundant food correlates negatively with the functional response for which population growth rate is zero. It also correlates negatively with the precociality index, i.e. the ratio of maturity levels at puberty and birth: the more precocial, the larger neonate size, the smaller reproduction rate, especially in restricted taxa such as mammals and cartilaginous fish. Like other traits, the population growth rate shows considerable segregation among taxa, where mammals have a relatively low rate, glires a relatively high rate among mammals, followed by marsupials; afrotherians have the lowest population growth rates.

* Corresponding author.
E-mail address: bas.kooijman@vu.nl (S.A.L.M. Kooijman).

https://doi.org/10.1016/j.ecolmodel.2020.109055
Received 7 November 2019; Received in revised form 24 February 2020; Accepted 25 March 2020
Available online 15 May 2020

1. Introduction

Physiologists focus on properties of individuals, whereas ecologists try to link those properties to population and ecosystem dynamics. Actual population dynamics suffers, however, from quite a list of complicating factors: the environment is changing in space and time, many factors affect survival (e.g. predators, pathogens, starvation), multiple types of resources exist (involving food selection), individuals interact (e.g. competition, flocking, territorial behaviour), migration and other forms of transport, dynamic weather conditions (daily and seasonal cycling of temperature, rainfall, drought, inducing torpor and migration) and even the boundaries of populations and ecosystem are typically poorly defined, hampering mass and energy balancing. While predator dynamics depend on prey availability, the latter depends on its resource dynamics as well and in no-time we have to deal with a huge number of variables, involving nutrient recycling at ecosystem level.

To disentangle this Gordian knot in a structured way, we here focus on what can be called 'potential population growth' for animals. For the potential population growth we assume homogeneous space and time, avoid defining population boundaries by working in densities of individuals, i.e. number of individuals per environmental surface area or volume, exclude feed-backs from the environment and focus on steady state situations, known as balanced growth. Despite its rather academic nature, potential population growth is an important ecological trait of a species, and still depends on environmental factors (temperature and substrate availability), as well as physiological and life history traits of species. Our position is that knowledge of the energetic basis of population growth is by no means sufficient for predictions of actual population dynamics, but such predictions do need this knowledge for being reliable.

The purpose of this paper is rather specialised: to study patterns in population growth potential among animal species in constant environments, where populations have a stable age and size distribution among its individuals, and to find links with the underlying energetics. We do this in the context of Dynamic Energy Budget (DEB) theory, which has been set up for this purpose (Kooijman, 1986b; Kooijman and Metz, 1984). DEB theory specifies how feeding, growth, reproduction and aging are inter-connected during the life cycle of an individual in a dynamically changing environment (Jusup et al., 2017; Kooijman, 2001; 2012; Ledder, 2014; van der Meer, 2006; Muller et al., 2019; Sara et al., 2014; Sousa et al., 2008; 2010). During its 40 years of development, this theory has been applied to many species, which invites to compare them on the basis of population performance.

A second purpose of this paper is to give background to the recently added 'Population traits' pages of the Add-my-Pet (AmP) collection (Marques et al., 2018; 2019). This collection of over 2000 animal species from all large phyla and all chordate orders (Anonymous, 2019a), concerns referenced data on energetics and life history, in combination with DEB parameters and implied properties that have been extracted from the empirical data.

This is the first paper that evaluates population traits based on energy parameters for many species that have been estimated from referenced data on energetics and life history at individual level, where the whole chain from empirical data to population traits can be checked in detail for all species, including code that has been used. This cannot be done with other models for individuals, since alternatives that specify individual dynamics thermodynamically will be too complex (Kooijman, 2020b).

Biodiversity presents a challenge in the context of population modeling. Most tetrapods produce a small number of (relatively large) offspring, but most ray-finned fish and invertebrates produce an enormous number of tiny eggs; if aging would be the only cause of death, the implied population growth rate of most ray-finned fish and invertebrates would be enormous as well. E.g. the ocean sunfish produces $3\,10^{10}$ eggs per year (Schmidt, 1921). Practice is, obviously, that only few of the many neonates make it to puberty. (The ocean sunfish is actually not abundant at all.) Tiny eggs in the aquatic environment are possibly an adaptation for dispersal, or risk minimisation if you wish, but the remarkable implication for fish is that the prey of the fish feeds on the early stages of the fish (Kooijman and Lika, 2014a), which comes with a high intrinsic hazard rate. Uncertainty about the dynamics of survival of fry motivated many fish biologists to bypass the problem and use demographic population models, where the smallest individuals have year-class one, assuming a recruitment rate that is independent of the standing crop, treating early life stage dynamics as black box. Assuming some constant (i.e. age and size independent) hazard to reduce numbers does not solve the problem, since this results in unrealistically few adults. What is needed here is a hazard rate that is high for young (small) individuals, and much lower for older (larger) ones; an element of the individual–environment interaction that became built into life histories during evolution.

Specifying such a hazard rate can be done in many ways, but, in the context of DEB theory, a single parameter-free way stands out, what is here called "thinning": The hazard rate is chosen such that the feeding rate of a cohort of neonates does not change in time, which fully determines the hazard rate, meaning that no extra parameters are involved. When individuals grow, they eat more, but this effect is exactly balanced by a reduction in numbers. The discussion section presents a further motivation for this choice.

This paper first presents an extended methods section, which serves as background information of the data presented on the population traits pages of the AmP collection (Anonymous, 2019a), on which the analysis in this paper is based. This section describes how properties of individual contribute to population growth. The first preliminary results of the analysis are reported in the results section, which starts with a discussion of the frequency distribution of population growth rates, illustrating the role of reproduction rate, puberty, and thinning. Then we explore how population growth rate depends on patterns in the covariation of parameter values that have been identified so far: body size-scaling, metabolic acceleration, waste-to-hurry, supply-demand spectrum and altricial-precocial spectrum. The discussion section places our findings in a wider context. The notation in this paper follows the DEB notation rules (Kooijman, 2020a).

2. Methods

2.1. Data

All data of all the 2027 species in the AmP collection at sampling date 2019/11/05 that has been analysed in this paper can be found on the AmP website (Anonymous, 2019a), including the references for the data, the code that has been used for the parameter estimation (Anonymous, 2019b; 2019c), all parameters, and many implied properties of the parameters. All entries in the AmP collection have been curated by a team of curators. The mean relative error of predictions for $\approx 3 \cdot 10^4$ data sets is just 0.07, which supports the realism of DEB models and parameter values as well as the generality and applicability of DEB theory. All code is documented and manuals are made available.

This paper is a study of patterns in parameter values. The data in each entry has a wide diversity among entries, basic life history data, such as age and size at life history events (birth, puberty, death), food intake, growth, reproduction, respiration. This diversity hampers direct comparison of species on the basis of data. While most entries have ultimate weight as data, relatively few entries have respiration, but all entries have predicted ultimate weight and predicted respiration. Moreover, data requires interpretation, which is done by DEB parameters, which all have clear connections with a single underlying physiological process.

The newly added population traits on the AmP website include: graphs of the survivor functions of the survival probabilities, and the stable age distribution at maximum and minimum food levels, population doubling times, and a list of statistics relating to the age and size

structure of the population, such as the mean values of powers of lengths, L^i, $i = 1, 2, 3$. The yield coefficients of the macro-chemical reaction equation for food to living and dead biomass at population level are also given, which can be useful in the study of mass turnover at ecosystem level. We here focus on first conclusions from this information provided in the AmP collection.

2.2. Model for individuals

Population growth in terms of densities of individuals in a constant homogeneous environment depends on survival and reproduction, while these processes depend on body size, making body growth relevant. For finite populations in a dynamic heterogeneous environment, a lot more becomes relevant as well, as indicated in the introduction.

The ten DEB models that are used in the AmP collection (Marques et al., 2018), are all simple extensions of the standard DEB model to account for extra life stages, metabolic acceleration, egg or foetal development. Detailed model specifications can be found in Appendix C; age zero corresponds with the start of embryo development, not with birth, since the models include embryo development. We describe aging below, since it is part of the model for individuals, and thinning in the subsection on population growth, since it reflects predation.

2.2.1. Aging

The aging module of DEB theory (Kooijman, 2010b; van Leeuwen et al., 2002) is based on the ideas that: (1) Damage inducing compounds (e.g. mitochrondrial DNA) are formed at a rate that is proportional to the use of dioxygen, which induce Reactive Oxygen Species (ROS); (2) Damage inducing compounds form damage compounds (e.g. modified proteins) at a constant rate; (3) The hazard rate is proportional to the concentration of damage compounds, and (4) Damage inducing compounds can produce more damage inducing compounds at a constant rate. The latter rate is typically low in ectotherms, but can be higher in endotherms (birds, mammals), with the effect that the survival probability due to aging remains high for a long period, relative to the life span, but then suddenly collapses.

An implication of this two-parameter DEB module for aging is that the popular empirical models by Weibull (1951) and Gompertz (1825) are both special cases at constant food, and on top of that, it links to energetics via respiration. It turned out to be difficult to decide which of these two empirical models fit survival data best (Ricklefs and Scheuerlein, 2002), but with the DEB aging module, there is no need for a choice, while this does not translate to more parameters. Dilution by growth keeps the hazard rate low and effects of caloric restriction are found to be well-captured by this module (van Leeuwen et al., 2002). Since larvae of holometabolic insects typically grow fast and reset structure during pupation, only imagos suffer from aging. Taxa like cephalopods sport programmed death, rather than aging; this process is modelled by the same equations to facilitate comparison.

2.2.2. Reproduction

The reproduction module of DEB theory is based on the ideas that: (1) allocation to maturation (i.e. increase in maturity) plus maturation maintenance is proportional to the mobilization of reserve, (2) maturation maintenance is proportional to maturity, (3) investment into maturation is redirected to filling of a reproduction buffer of reserve as soon as maturity reaches the puberty threshold level, and (4) the reproduction buffer is converted to eggs or fetuses at reproduction events, based on species-specific buffer handling rules, which can depend on physiological and/or environmental cues. The maximum reproduction rate $\dot{R}_m$ is the mean number of offspring (eggs/foetuses) per time averaged over many reproduction event intervals for an individual of maximum size at abundant food.

Reproduction is here taken to be continuous, which is obviously an approximation. The fact that the reproduction buffer first needs to accumulate enough to produce an offspring (egg or foetus) reduces the specific population growth rate because of the involved waiting time, but its impact rapidly decreases for increasing age at puberty (Kooijman, 2010b, Fig 9.8). Since this error is small relative to that induced by another, more complex, fact, it is ignored. This fact is that eggs/foetuses are frequently produced in clutches/litters of several to many offspring, frequently in synchronisation with the seasons, involving much longer waiting times. Even this fact is ignored, since it is species-specific, and frequently depends on the location in the geographic area of the species and on local climate.

In gonochoric heterogamous species, males are taken into account by halving the reproduction efficiency κ_R, on the assumptions that the sex ratio is 1:1 and male and female eggs/foetuses are equally costly; only females directly contribute to the production of offspring. Reproduction efficiency only affects the conversion of the contents of the reproduction buffer to offspring, so the idea is that half of it is 'lost' for the production of males. This is not done for hermaphroditic species, nor for parthenogenic species. Simultaneous hermaphrodites have already a reduced κ_R to account for sperm production. Sequential hermaphrodites have no reduced κ_R, but the age at first egg production does not coincide with puberty for protandric hermaphrodites (i.e. first male, then female).

2.2.3. Body growth

The growth module of DEB theory is based on the assumptions that: (1) allocation to growth (i.e. increase of structure) plus somatic maintenance is proportional to the mobilization of reserve, and (2) somatic maintenance is proportional to structure.

The relevance of body growth for population growth is that feeding, in DEB theory, is linked to surface area, and reproduction is linked to feeding. We discuss the effect of body size on population growth in the section on body size scaling.

2.3. Population growth

As known since Malthus (1798), any population will eventually grow exponentially in a constant environment, due to the fact that offspring follow the same reproduction and survival pattern as the parents. The specific population growth rate, $\dot{r}_N$ (also called the intrinsic rate of increase, or the *per capita* growth rate, or Malthusian parameter) can be computed by solving the characteristic (also called the Euler-Lotka or renewal) equation (Kot, 2001; Pielou, 1969; de Roos, 1997). For individuals of age a, survival probability S and reproduction rate $\dot{R}$, the characteristic equation is

$$1 = \int_0^\infty S(a)\dot{R}(a)\exp(-\dot{r}_N a)\,da \tag{1}$$

We also used Eq. (1) to obtain the scaled functional response f_0 at which by solving it in scaled function response f, while fixing $\dot{r}_N = 0$, where S as well as $\dot{R}$ depend on f. This statistic quantifies the minimum environmental quality for long-term survival, relative to the food-searching abilities of the species. For $f > f_0$ the population grows to infinity, for $f < f_0$ the population goes extinct. While thinning does not affect growth or reproduction rate, given food availability via f, it does affect f_0, since the effect of thinning has to be compensated by reproduction, given $\dot{r}_N = 0$.

For the standard DEB model, the thinning hazard amounts to $\dot{h}(a) = \dot{r}(a)\frac{2}{3}$, where $\dot{r}(a) = \frac{d}{da}\ln L(a)^3$ is the specific growth rate of structure of an individual of age a and structural length L. This can be seen from the feeding rate of a cohort of N_0 neonates, $\dot{J}_X^N(a) = N_0 S(a)\{\dot{J}_X\}L^2(a)$, where $\{\dot{J}_X\}$ is the surface-area specific feeding rate of an individual and L its structural length. By our definition of thinning, this cohort feeding rate should not change in time, so $\frac{d}{da}\dot{J}_X^N = 0$, while $\frac{d}{da}L^3 = L^3\dot{r}(a)$ (by definition of the specific growth rate of structure) and $\frac{d}{da}S = -S\dot{h}(a)$ (by definition of the hazard rate). The

factor $\frac{2}{3}$ in the expression for the thinning hazard originates from surface area being proportional to L^2, and volume to L^3, for isomorphs. For V1-morphs, i.e. individuals whose surface area increases proportional to volume, which is a temporary stage in the family of a- and h-models (Marques et al., 2018), $\{\dot{J}_X\}$ is not a constant, but is proportional to L (Kooijman, 2014), the hazard rate for thinning amounts to $\dot{h}(a) = \dot{r}(a)$. Species that sport metabolic acceleration temporarily behave as V1-morphs; this occurs only in particular taxa, typically with larval stages.

In this paper thinning was applied to entries for which ultimate reproduction of a fully grown adult $\dot{R}_i > 1$ d^{-1}, because absence of thinning lacks realism for these species as the population would grow theoretically at enormous rates with only aging as cause of death (see introduction). We found that our results are not sensitive to the value of this threshold for $\dot{R}_i$. The underlying idea is that species with many (tiny) eggs are adapted to intense predation during the early stages; they typically do not allocate more (mobilised reserve) to reproduction, compared to species with large eggs, which links egg size directly to reproduction rate.

2.3.1. Numerical methods and implementation

The computations of the population characteristics have been done for all > 2000 species of the AmP collection, with function "AmPtool/curation/prt_my_pet_pop" of AmPtool (Anonymous, 2019b), which uses DEBtool (Anonymous, 2019c) intensively. Both freely downloadable software packages are written in Matlab, and the results are made available under 'population traits' for each species on the AmP website (Anonymous, 2019a). Function `prt_my_pet_pop` enables the setting of temperature, scaled function response, stage-specific background hazard rates, on top of the optional thinning hazard and the obligatory aging hazard. This function can be used for species that are not yet added to the AmP collection, but also for existing ones. In the latter case, the function detects if males and females differ in parameter settings and the population characteristics take this into account. We found a few cases where the scaled functional response that results in $\dot{r}_N = 0$ for females, is too low for males to reach puberty.

The specific population growth rate $\dot{r}_N$ is calculated by solving the characteristic Eq. (1). Integration of the characteristic equation has been continued till the survival probability becomes less than 10^{-6}, using an event handler in combination with a Runge-Kutta-4,5-method with relative and absolute tolerance of 10^{-9}. These small tolerances turned out to be necessary for numerical stability. We are looking for a non-negative solution for $\dot{r}_N$, since shrinking of the population cannot be a steady state; if the solution exists, it is unique.

The solution has been found with a bisection method for each of the AmP entries, using the upper boundary $\dot{r}_N^m$ that is specified by $\exp(-\dot{r}_N^m a_p) = \dot{r}_N^m/\dot{R}_m$, where a_p is the time since birth at puberty ($\dot{R}(a) = 0$ for $a < a_p$) and $\dot{R}_m$ the maximum reproduction rate (at abundant food), with eternal survival (Kooijman, 2010b, Eq. (9.21)). This follows directly from the characteristic equation $1 = \dot{R}_m \int_{a_p}^{\infty} \exp(-\dot{r}_N^m a)\, da$. The solution for $\dot{r}_N^m$ was again found with a bisection method, now using $\dot{R}_m$ as upper boundary, but this is fast because no integration is involved.

2.3.2. Stable age distribution

The population traits pages of the AmP collection show the stable age distribution that underlie the specific population growth rate. The survivor function of the stable age distribution is given by

$$S_a(a) = \frac{\int_a^{\infty} \exp(-\dot{r}_N t) S(t)\, dt}{\int_0^{\infty} \exp(-\dot{r}_N t) S(t)\, dt} \tag{2}$$

It only applies when the population grows exponentially, i.e. balanced growth. An implication of the stable age distribution is that the relative frequency decreases as function of age. This rarely occurs in reality, since balanced growth rarely occurs in nature. Yet it controls mass turnover at population level. Graphs of the survival probability $S(a)$ and the survivor function of the stable age distribution $S_a(a)$ can be found in the AmP website (Anonymous, 2019a) for all species, with and without thinning.

2.4. Macro-chemical reaction equation

The conversion of food to living and dead biomass and faeces at the population level can be summarized by the macro-chemical reaction equation

$$\mathrm{X} + Y_{OX}\,\mathrm{O} \rightarrow Y_{VX}\,\mathrm{V} + Y_{VX}^{\dagger}\,\mathrm{V}_{\dagger} + Y_{EX}\,\mathrm{E} + Y_{EX}^{\dagger}\,\mathrm{E}_{\dagger} + Y_{PX}\,\mathrm{P} + Y_{HX}\,\mathrm{H} + Y_{NX}\,\mathrm{N} + \mu_{TX}$$

for food X, living structure V, dead structure $\mathrm{V}_{\dagger}$, living reserve E, dead reserve $\mathrm{E}_{\dagger}$, faeces P, dioxygen O, water H and nitrogen waste N, which can be ammonia, urea or uric acid, depending on the taxon at phylum or class level. Notice that these symbols stand for types, not for quantities. The yield coefficients Y depend on the population growth rate $\dot{r}_N$; that for food has been chosen equal to one as reference. Yields are ratios of fluxes; Y_{OX} is taken negative since dioxygen disappears, rather than appears. These mass fluxes are expressed in C-mole per time (one mole of glucose corresponds with 6 C-moles of glucose) and can, like energy fluxes, all be written as cubic polynomials in structural length in DEB models (Kooijman, 2010b, Section 4.3.1). The yield of heat on food, μ_{TX}, is here expressed as Joules per consumed C-mole of food, time dropping out in the ratio.

The reaction equation only involves the 4 most abundant chemical elements in biomass. Extension to include additional elements is straight-forward, as long as we also include one mineral for each extra element that contains that element. We exclude water loss that results from evaporation, which involves a drinking rate to compensate, since this involves environmental details. The water balance is discussed in (Kooijman, 2010b, Section 4.6). The yield of water in the macro-chemical reaction equation only concerns metabolic water. The reaction equation does not specify fermentation products (Kooijman, 2010b, Section 4.9.1), assuming that dioxygen is not rate limiting and food is the only component that is possibly limiting. Situations where more than one resource is potentially limiting are discussed in (Kooijman, 2010b, Chapter 5).

Appendix A shows how the yield coefficients depend on the population growth rate. Values for the yield coefficients and heat can be found on the AmP website (Anonymous, 2019a) for all species.

The parameter values of males can differ from that of females, in which case the web-page reports the coefficients of two macro-chemical reaction equations.

The package AmPtool (Anonymous, 2019b), in combination with DEBtool (Anonymous, 2019c), can generate similar local html-pages where the user can set the background hazard (which was set to zero for the web-pages) and modify the setting of other parameters to study the effects on population traits (Anonymous, 2019a, dropdown `APPLICATIONS`).

3. Results

The script-files for all figures are available in the supporting information. The AmP data (i.e. all parameters, individual and population traits for all species) can be downloaded from the AmP website (Anonymous, 2019a, dropdown `COLLECTION`), and the required AmPtool (Anonymous, 2019b) and DEBtool (Anonymous, 2019c) from GitHub. The choice of taxa and markers can be modified in the script files. The scripts produce Matlab-figures and clicking on a marker in these figures shows the corresponding species-name. The AmP-website can be used to check traits for that species and the empirical data from which these traits were derived.

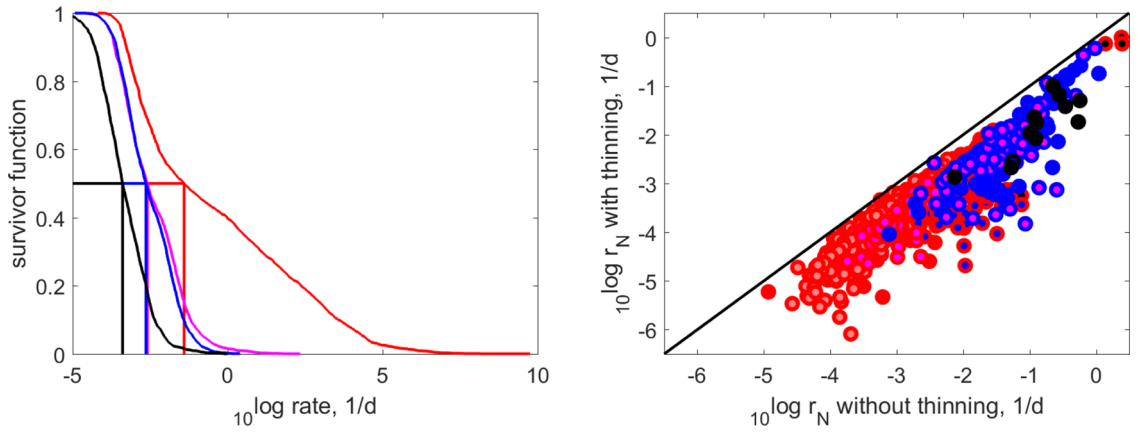

Fig. 1. Left panel: The survivor functions and medians for (from right to left): the maximum reproduction rate $\dot{R}_m$ (red), the ceiling $\dot{r}_N^m$ for the specific population growth rate (magenta), and the specific population growth rate $\dot{r}_N$ without (blue) and with thinning (black), for the 2027 species in the AmP collection (but semelparous species were excluded in $\dot{R}_m$ as such a rate is not defined for them). **Right panel**: the specific population growth rate $\dot{r}_N$ with thinning, as function of that without thinning. The line of equal rates has been indicated; colour coding as in Fig. 2. All calculations performed at $f = 1$ and all rates are corrected for 20 ˚C. (For interpretation of the references to colour in this figure legend, the reader is referred to the web version of this article.)

3.1. Effects of reproduction, puberty and thinning

Fig. 1, left, shows 4 curves, that will be discussed from right to left, step-wise involving more traits. Red curve (right curve): If survival would be eternal, $S(a) = 1$, and reproduction at maximum for all ages (including embryos), $\dot{R}(a) = \dot{R}_m$, the specific population growth rate equals maximum reproduction rate, . This can be seen from Eq. (1). Under these conditions the red curve not only represents the maximum reproduction rate, but also the maximum population growth rate.

The magenta curve in Fig. 1 shows that the ceiling for the (maximum) population growth rate $\dot{r}_N^m$ is quite a bit smaller, while the only difference with the red curve is that reproduction is zero till puberty (so survival is still eternal).

Blue curve: The (maximum) population growth rate itself (without thinning), is slightly smaller than its ceiling, while the difference with the magenta curve is that reproduction just after puberty is less than maximum due to growth during the adult phase, and survival is subjected to aging. This means that the effect of age at puberty is much more important than the effect of aging or the fact that most species still grow and increase their reproduction rate after puberty.

Fig. 1 shows that the magenta curve for the ceiling $\dot{r}_N^m$ and the blue one for the population growth rate itself $\dot{r}_N$ are almost identical for rates smaller than the median rates. The 450 species of birds in the AmP collection at 2019/11/05 play a relatively large role in this similarity: they have few (big) offspring (so small $\dot{r}_N$), hardly grow as adults, and have a long life span. So birds actually approximate the assumptions behind the ceiling $\dot{r}_N^m$. For rates larger than the median rates, the curves for $\dot{r}_N^m$ and $\dot{r}_N$ deviate somewhat. The 502 species of ray-finned fish play a relatively large role in the explanation: they produce many tiny eggs, so have a large $\dot{r}_N$ (without thinning), and grow substantially during reproduction (i.e. slowly increasing their reproduction rate with age). The effect that reproduction rate increases with age is thus somewhat more relevant for population growth for this taxon.

The black curve (left curve) in Fig. 1 shows that the mean effect of thinning is substantial. Since the black curve (with thinning) is almost parallel to the blue one (without thinning), while the rates are log-transformed, the effect of thinning in practice means a reduction by an almost constant factor (on average). Not all species survive thinning, i.e. the characteristic equation does not have a solution, even for $f = 1$, for 228 of the 2027 species. These species tend to have a juvenile period that is a substantial fraction of the life span, but we failed to detect simple causes.

Fig. 1 shows in the right panel that the effect of thinning is rather species-specific, varying from strong to almost no effect. Thinning has relatively little effect on large-bodied species, because they have a small specific growth rate of structure, so a small thinning hazard.

3.2. Body size scaling

The data covers the full range of body sizes among extant animals, from the hairy back with a maximum body weight of $8{\cdot}10^{-8}$ g to the blue whale of $1.6 \cdot 10^{8}$ g. This range of a factor $2 \cdot 10^{15}$ coincides with predictable shifts in parameter values that depend on the physical interpretation of parameters, contrary to the other co-variation rules

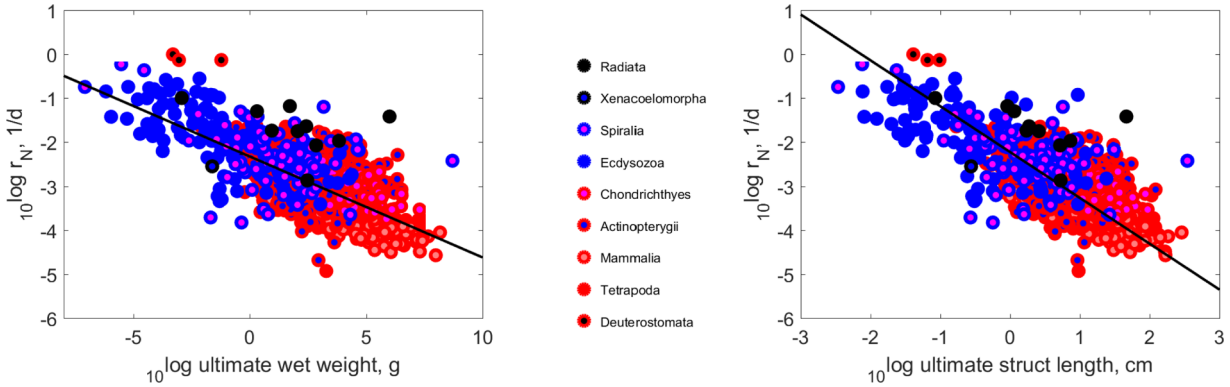

Fig. 2. The specific population growth rate, $\dot{r}_N$, at 20 ˚C, as function of predicted maximum body weight (**left panel**) or structural length (**right panel**). Thinning is applied if $\dot{R}_i > 1\ d^{-1}$. The first principal component is indicated, which has slope -0.23 and -1.09, respectively. All calculations were performed at $f = 1$.

discussed in the next subsections, which involve physiological, ecological and evolutionary adaptations. The *a priory* rules for the co-variation of DEB parameters are based on the ideas that (1) parameters are either intensive or extensive, given their physical interpretation, (2) appropriate ratios of extensive parameters are intensive, and (3) maximum structural length depends on three parameters, one of which is extensive, namely, the specific maximum assimilation. The co-variation rules imply that the latter is proportional to maximum structural length and that all parameters can be linked to each other, including traits that can be written as functions of DEB parameters (Kooijman, 1986a; 2010b).

These rules predict that maximum population growth rate decreases with maximum structural length to the power somewhat larger than 1 (Kooijman, 1986a; 2010b). Our present finding of a scaling exponent of -1.09 for length, or -0.23 for body weight among animal species is consistent with the expectations, see Fig. 2. Maximum size is an implied trait of energetics (Lika et al., 2019) and large-bodied species tend to have relatively more reserve which is why body weight is more than proportional to cubed structural length.

A scaling power with body weight of -0.20 has been found (Brown et al., 2007; Savage et al., 2004) for a small set of species (algae, zooplankton and fish), which is numerically close to our results, but they explained it as a result of respiration. We now discuss why our explanation differs.

Fig. 3 shows the (predicted) weight-specific respiration as function of the (predicted) ultimate wet weight at 20 °C and $f = 1$. So the scaling is the same as for the specific population growth rate of the data in the AmP collection; see the discussion section.

Absolute growth of structure typically increases after birth and then decreases, becoming zero when an individual is fully grown. Fig. 3 shows that the maximum population growth rate roughly equals the specific growth rate of structure at maximum growth, see the Appendix B for its relationship with maximum specific growth of structure. This appendix also shows that the specific growth rate of structure at maximum growth is 1.5 times the von Bertalanffy growth rate (after metamorphosis). The finding of the equality of rates is remarkable, because population growth relates to survival and reproduction, not to growth of structure directly. We come back to this in the discussion. Endotherms tend to have a lower population growth rate, compared to ectotherms, despite the fact that thinning has been applied to fast-reproducing species, so most ectotherms.

3.3. Metabolic acceleration

About a third of the AmP species sport metabolic acceleration: a temporary deviation from isomorphy, where surface area is proportional to volume, rather then volume$^{2/3}$ (Kooijman, 2014; Kooijman et al., 2011). It is quantified by the ratio of structural length at the end and the start of acceleration, called the acceleration factor s_M. Both start and end are triggered by exceeding maturity levels. As result, the specific maximum assimilation and energy conductance, which control the mobilisation rate of reserve, increase proportional to length during acceleration period. This means that both parameters are multiplied by the acceleration factor to convert the situation before to after acceleration. The ability to accelerate is the backbone of the family-structure of DEB models, that are used in the AmP collection (Marques et al., 2018).

We found no clear link between the population growth rate and the acceleration factor. This is not shown to reduce the number of figures.

3.4. Waste-to-hurry

The waste-to-hurry pattern in co-variation of parameter values states that specific assimilation increases with specific maintenance in small-bodied species that are adapted to short-lasting peaks in food-abundance, coupled to torpor (and substantial death) during low-food intervals. This comes with a high maximum growth and reproduction (Kooijman, 2013), not only in theory, but also in data. It is an implication of the κ-rule of DEB theory, which states that a fixed fraction of mobilised reserve is allocated to soma (growth of structure plus somatic maintenance). It, therefore, seems natural to expect that waste-to-hurry also comes with a high specific population growth rate $\dot{r}_N$. Fig. 3 shows, however, that this holds for spiralia and ecdysozoa (i.e. 95% of all animal species), but not so clearly for tetrapods. The reason for this possibly relates to the fact that specific somatic maintenance $[\dot{p}_M]$ also appears to co-vary with the specific maturity at puberty, $[E_H^p]$, as shown in Fig. 4. An increase of maturity at puberty typically increases age at puberty, and so decreases population growth. While tetrapods tend to have high maturity levels at birth and puberty, combined with a large ultimate body mass, invertebrates have the opposite. Quite a few parameters are involved, however, which complicates the analysis. Why waste-to-hurry is impossible for large-bodied species is explained in Augustine et al. (2019b). So the waste-to-hurry strategy more frequently occurs among small-bodied species.

3.5. Supply-demand spectrum

Demand-species have 'pre-programmed' growth and reproduction trajectories, and eat what they need, while supply-species are much more flexible (Lika et al., 2014); demand-species evolved from supply-species. The supply-stress s_s quantifies the position of species in the supply-demand spectrum and is defined as the maturity maintenance $\dot{p}_J$

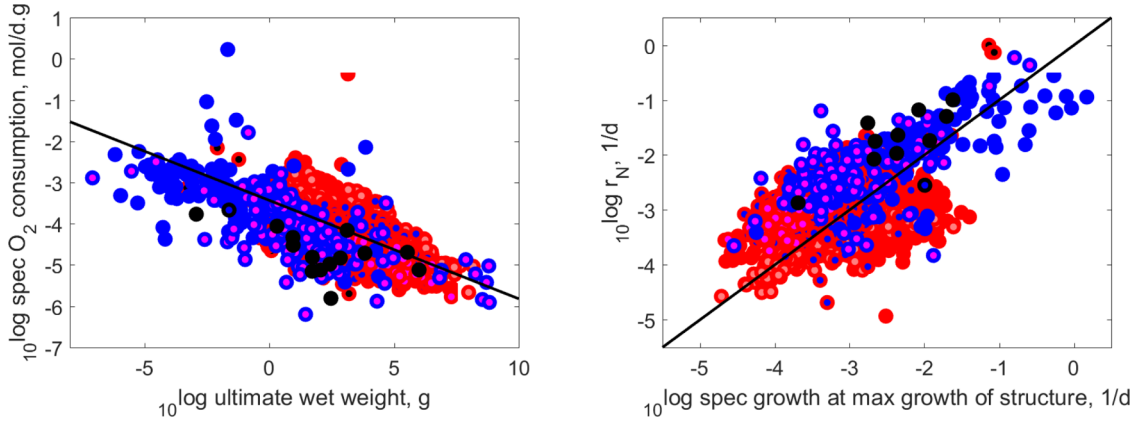

Fig. 3. Left panel: The predicted weight-specific respiration rate as function of the predicted ultimate wet weight. The first principal component is indicated, which has slope -0.24. **Right panel**: The specific population growth rate, $\dot{r}_N$, as function of the specific growth rate of structure at maximum growth; thinning is applied if $\dot{R}_i > 1$ d^{-1} and the line of equal rates is indicated. All calculations performed at $f = 1$ and all rates are corrected for 20 °C; colour coding as in Fig. 2.

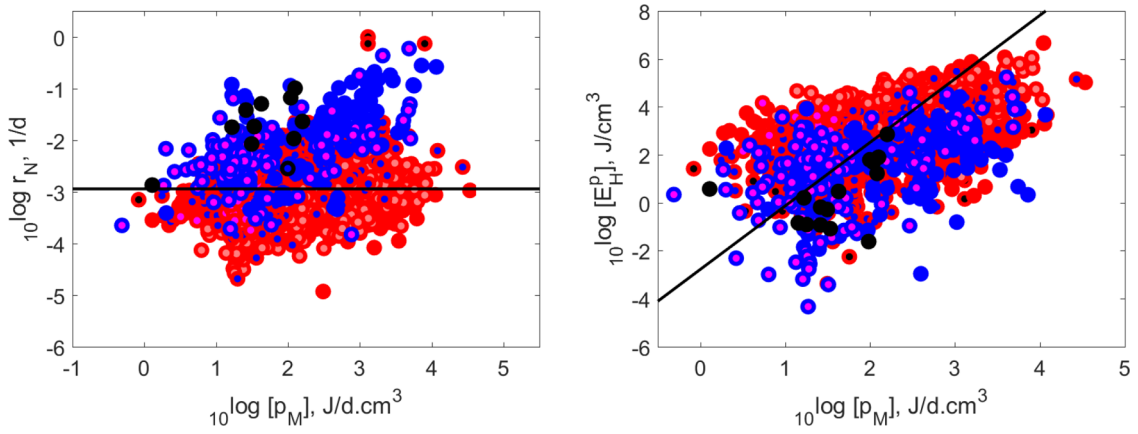

Fig. 4. Left panel: The specific population growth rate, $\dot{r}_N$, as function of specific somatic maintenance $[\dot{p}_M]$. Thinning is applied if $\dot{R}_i > 1\ d^{-1}$. The line is the first principle component with slope 0. **Right panel**: The specific maturity at puberty, $[E_H^p]$, as function of $[\dot{p}_M]$. The line is the first principle component with slope 2.65. All calculations performed at $f = 1$ and all rates are corrected for 20 ˚C; colour coding as in Fig. 2.

times the squared somatic one $\dot{p}_M$, divided by cubed assimilation $\dot{p}_A$, so $s_s = \dot{p}_J \dot{p}_M^2/\dot{p}_A^3$. It is body size independent and can take values between 0 and $2^2/3^3$, in the context of DEB theory. Endotherms (i.e. birds and mammals) turn out to have a high supply stress (which makes them demand-species), reptiles, amphibians and cartilaginous fish have intermediate values, ray-finned fish have lower values, while insects are extreme supply-species. Demand-species differ in quite a few properties from supply-species (Lika et al., 2014), and tend to have a high (scaled) functional response to reach puberty.

The scaled functional response that is required to reach puberty, $f_{\min}$, has a direct relationship with the supply-stress, s_s, and the allocation fraction κ of mobilised reserve to soma, which can be predicted on *a priori* grounds (Lika et al., 2014). Species parameter sets reveal only tiny deviations from the surface (s_s, $f_{\min}$, κ), specified by supply-stress $s_s = f_{\min}^3 \kappa^2 (1 - \kappa)$. These deviations are caused by the amount of metabolic acceleration being (somewhat) dependent on the scaled functional response.

The scaled functional response f_0 at which specific population growth rate equals zero, $\dot{r}_N = 0$, is very close to one required to reach puberty $f_{\min}$. Fig. 5 shows that $\dot{r}_N$, at abundant food, is decreasing for increasing f_0. This might not come as a complete surprise, since a high $f_0 \simeq f_{\min}$ means a high supply-stress s_s, or a low demand-stress $s_d = \frac{4}{27} - s_s$, while birds and mammals dominate demand-species and have a relatively large body size, so a low population growth rate. The observation is ecologically important and directly relates to the supply-demand spectrum.

The specific growth rate tends to decrease somewhat for increasing allocation fraction κ to soma, see Fig. 6. A high value of κ, means a low fraction of mobilised reserve invested in maturation (so high age at puberty), and reproduction (so low reproduction rate), which leads to a low population growth rate. We did not find clear relationships between $\dot{r}_N$ and s_s, which is surprising given the relationship between s_s and $f_{\min}$, being close to f_0.

We can think of f_0 as a requirement for environmental quality, but one that is strongly modified by the small half-saturation constant for demand-species. On top of that, endotherms sport another adaptation, up-regulation of assimilation associated to reproduction events, to escape the environmental quality restrictions, to some extent. This is not part of the standard DEB model, but included in more advanced DEB models.

The segregation of taxon-specific properties can also be seen in Fig. 5, showing that mammals have a relatively low population growth rate; the gliriformes (rodents and hares) have the highest population growth rate among mammals, followed by the marsupials, while afrotheria have the lowest, but the blue whale has the lowest population growth rate of all.

3.6. Altricial-precocial spectrum

The precociality index s_H^{bp} quantifies the position of species in the altricial-precocial spectrum and is defined as the ratio of the maturity at birth E_H^b and puberty E_H^p, so $s_H^{bp} = E_H^b/E_H^p$. This index takes values between 0 (extreme altricial) and 1 (extreme precocial). Since *a priory* covariation rules predict that both maturities scale with cubed maximum structural length, this index is expected to be independent of body size. Augustine et al. (2019a) confirmed this expectation for mammals, but

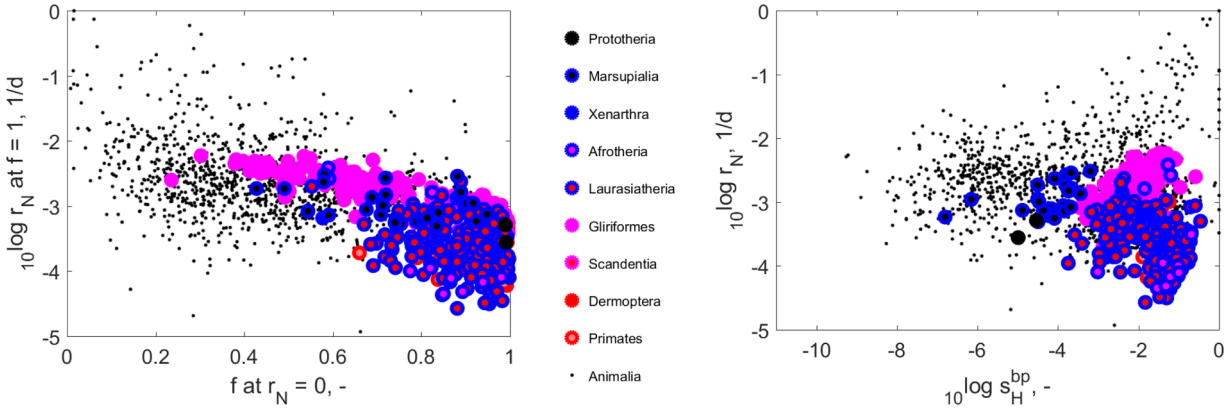

Fig. 5. The specific population growth rate, $\dot{r}_N$, at 20 ˚C and abundant food ($f = 1$), as function of the minimum functional response f_0 (**left panel**) and of the precociality index s_H^{bp} (**right panel**). Thinning is applied if $\dot{R}_i > 1\ \mathrm{d}^{-1}$.

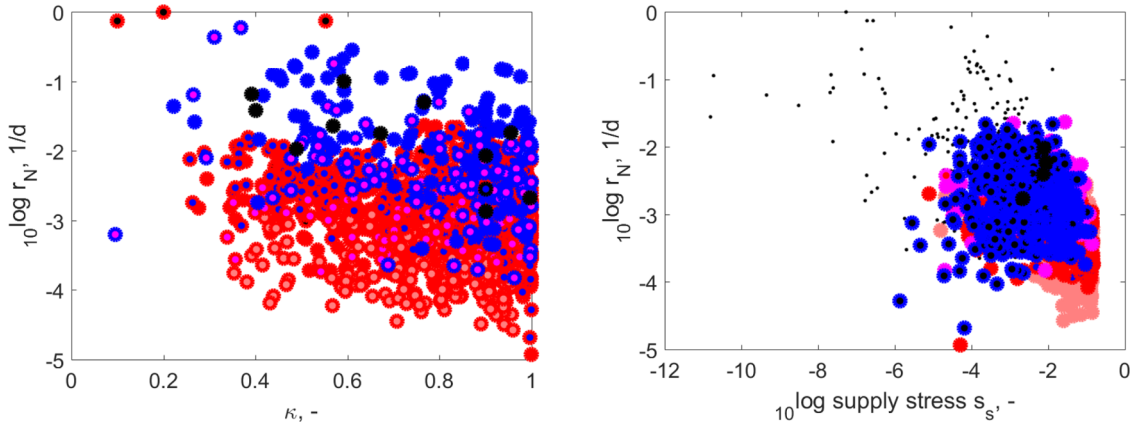

Fig. 6. The specific population growth rate, $\dot{r}_N$, as function of allocation fraction κ of mobilised reserve to soma (left) and of supply-stress s_s (right). Thinning is applied if $\dot{R}_i > 1$ d^{-1}. All calculations performed at $f = 1$ and all rates are corrected for 20 °C; colour coding as in Fig. 2.

s_H^{bp} tends to decrease with maximum body weight for other animal taxa. Fig. 5 shows that $\dot{r}_N$ for mammals and cartilaginous fish tend to decrease somewhat with s_H^{bp}, but for invertebrates and ray-finned fish this is even much less clear. A possible explanation for the complex relationship is that an increase in s_H^{bp}, so in size at birth relative to puberty (maturity co-varies with size Augustine et al., 2011), reduces reproduction rate, but also shortens waiting time till puberty, which increases $\dot{r}_N$.

4. Discussion and conclusions

A natural question that one might have is to what extent the reported population growth rates are reliable. We stated in the introduction that homogeneous space, constant food density and temperature, absence of causes of death (apart from aging and thinning) do not occur in nature. Moreover, feed-backs from the environment prevent continued population growth, so we cannot test reliability with empirical data. Potential population growth rates depend on a number of parameters at the individual level and their accuracy depends on the data that was used for estimation. We do not see possibilities to test reliability, but can point to another implied property, that has been measured in a minority of the AmP entries: respiration, which also depends on several parameters. In the cases were it was measured, the fit is good, while the parameters are consistent with related species for which respiration was not measured.

Thinning may (partly) solve a problem for (theoretical) population dynamics, which is implied by DEB theory (van der Meer, 2016): in homogeneous space and time, individuals in an Individual-Based-Model (IBM) tend to synchronise their life cycles, where the young generation out-competes the adults (Kooijman, 2010b). Upon reaching puberty synchronously, the newly produced offspring again out-competes the existing generation. The fact that food shortage impacts growth more the larger the individual, induces synchronisation; this is a structural property of DEB models for isomorphs, i.e., organisms that do not change shape during ontogeny. The reason is that the scaled functional response needs to exceed structural length as fraction of the maximum to grow, so the larger the individual, the higher the minimum food level must be. This behaviour poses problems for the theoretical study of population properties as implied by DEB theory. We need to understand model implications in simple situations before we can interpret their implications on more realistic situations. The reduction of the synchronisation effect motivated us to link thinning to food consumption. We know that synchronisation can also be reduced by allowing for scatter in parameter values among individuals (Kooijman, 2010b) and spatial or temporal heterogeneity, but these routes complicate the mathematical analysis.

We see the progress reported in this paper as a first step in a long series. With use of the reported yield coefficients, we will eventually be able to test popular assumptions, such as the maximisation of entropy dissipation at the population level (Sousa et al., 2006). The AmP collection was already instrumental to test another popular assumption, that of the maximization of reproductive output, which was found to be strongly at odds with evidence (Kooijman and Lika, 2014b). Meanwhile the AmP collection grew from 276 in that paper, to 2027 species at present, only further supporting its conclusions. We now also better understand why the allocation fraction to soma, and so to reproduction, follows a beta distribution among species (Lika et al., 2019).

We found that the specific population growth rate $\dot{r}_N$ and the weight-specific respiration scale with maximum body weight to the power -0.23 and -0.24, respectively. These values are very close to Kleiber's empirical value -0.25 for weight-specific respiration (Kleiber, 1932), and in view of the scatter in data, these values can considered to be the same. DEB theory explains both types of scaling (Kooijman, 1986a; 2010b), but also shows that the relationship between population growth and respiration is only incidental. Population growth depends on reproduction and survival. Reproduction, treated as export of wrapped reserve in DEB theory, hardly contributes to respiration, since the chemical composition of freshly laid eggs and reserve are the same, whereas the contribution of feeding (for fuelling egg production) to respiration was experimentally excluded in Kleiber's data. We showed that the second most important determinant of population growth is age at puberty. It also does not have a straightforward relationship with respiration.

We believe that the similarity of these and other scaling powers hampered the evolution of ecological thinking substantially, since the popularity of linking a wide variety of quantities directly to metabolic rate with allometric functions (Huxley, 1932). We see metabolism as a network of interrelated processes, and the quantification of fluxes through this network by a single number has strong limitations.

Is the similarity in scaling of specific population growth and respiration with maximum body mass then purely coincidental? We suggest that it might be caused by the equality of specific population growth with the specific growth of structure at maximum growth, as reported in the results-section; the latter has a much more direct relationship with respiration via growth overheads. What then causes the equality of these growth rates? If we look at a population of unicellulars, which multiply by division, then growth of individuals can be accurately approximated by that of V1-morphs. This is because the detailed morphology of the growth curve does not matter much if cell structural volume maximally doubles since birth. For a population of unicellular V1-morphs, the specific population growth rate actually equals the specific growth rate of structure conceptually (Kooi and Kooijman, 1994), since for V1-morphs the difference between populations and individuals disappears. Since animals evolved from

unicellulars, the equality of both specific growth rates might be an evolutionary relict. While body growth controls population growth in unicellulars, with a limited role of survival, reproduction — including age at puberty — and a more complex role of survival controls population growth in animals, but it seems that the average population growth rate among species remained unaffected in the transition. Notice that maximum specific growth rate equals the specific growth rate at maximum growth in dividing unicellulars, but not so in animals, where the latter rate took control, if our interpretation holds.

While conversion efficiency from food to biomass at the individual level is controlled by physiological factors, as quantified by DEB theory, that at population level is controlled by ecological factors, where the role of physiology is reduced to setting boundary conditions (Kooijman, 1992). The yield coefficients of the macro-chemical reaction equation are sensitive to the background hazard, as can be explored using the DEBtool (Anonymous, 2019c) and AmPtool (Anonymous, 2019b) packages.

Conclusions of this research are as follows.

- Some 11% of the species do not survive thinning.
- The maximum population growth rate about equals the specific growth rate of structure at maximum growth for most taxa, if thinning applies for fast-reproducing species, but the scatter is substantial. The match is exact for organisms that divide, rather than reproduce, and we suggest the equality for animals to be an evolutionary relict.
- The maximum population growth rate decreases approximately with maximum weight to the power -0.25 among species, as predicted *a priori*. This is the same as for weight-specific respiration, which is also predicted *a priori*, but these predictions show that there is no direct link between population growth and respiration.
- The scatter in population growth rates at the reference temperature, for a given specific growth rate of structure, amounts to a factor 100 and is higher for invertebrates, compared to vertebrates, even if thinning applies for fast-reproducing species.
- The waste-to-hurry strategy of increasing growth and reproduction by increasing assimilation and somatic maintenance simultaneously translates in a clear positive relationship between somatic maintenance and population growth for ecdysozoa and spiralia, but not for tetrapods. We present the explanation: the maturity level at puberty depends on maintenance for tetrapods.
- The scaled functional response at which the population growth rate is zero is very close to that at which puberty can just be reached in absence of thinning, and somewhat increased in presence of thinning. The specific population growth rate decreases for increasing for minimum functional response. We present an explanation.
- Specific population growth rate decreases for increasing precociality index for mammals and cartilaginous fish, but not so for invertebrates and ray-finned fish. We suggest an explantation.
- Like other traits, the population growth rate shows considerable segregation among taxa, where mammals have a relatively low rate, glires a relatively high rate among mammals, followed by marsupials, and afrotherians the lowest ones.
- We found a new interpretation for the von Bertalanffy growth rate: 1.5 times this rate equals the specific growth rate at maximum growth.

Acknowledgements

SA was supported by the Norwegian Science Council (NFR 255295). NM was supported by the Croatian science foundation (HRZZ) project AqADAPT (no. IP-2018-01-3150). We want to thank all who contributed to the AmP collection and two anonymous reviewers, whose comments considerably improved the paper.

Appendix A. Macro-chemical reaction equation

The (state-dependent) macro-chemical reaction equation at individual level is discussed in (Kooijman, 2010b, Section 4.3), but at population level we need to account for dead biomass production as well and for the age distribution (i.e. taking a weighted mean over all ages). The macro-chemical reaction equation at population level reads

$$\mathrm{X} + Y_{OX}\,\mathrm{O} \rightarrow Y_{VX}\,\mathrm{V} + Y^{\dagger}_{VX}\mathrm{V}_{\dagger} + Y_{EX}\,\mathrm{E} + Y^{\dagger}_{EX}\mathrm{E}_{\dagger} + Y_{PX}\,\mathrm{P} + Y_{HX}\,\mathrm{H} + Y_{NX}\,\mathrm{N} + \mu_{TX}$$

for food X, living structure V, dead structure $\mathrm{V}_{\dagger}$, living reserve E (including reproduction buffer), dead reserve $\mathrm{E}_{\dagger}$ (including dead reproduction buffer), faeces P, dioxygen (O_2) O, water (H_2O) H and nitrogen waste N, which can be ammonia (NH_3), urea (CH_2ON_2) or uric acid ($CH_{4/5}O_{3/5}N_{4/5}$), depending on the taxon at phylum or class level (see function `get_N_waste` of DEBtool Anonymous, 2019c). The last symbol μ_{Tx} stands for the yield of heat on food (in Joules per C-mole).

We here derive how the yield coefficients (C-mole per C-mole) in the macro-chemical reaction equation depends on the population growth rate for the std-model. For this derivation we need structural length L, reserve E and reproduction buffer E_R as functions of age a. They are model-dependent and specified in Appendix C for all models.

First we need a couple of chemical parameters. These parameters are set at default values, but can be overwritten by the user, are stored for each entry, and reported on the parameter-pages. The stored values have been used for computation of the yield coefficients, as reported on the AmP population traits-pages.

The default values for the chemical indices (i.e. elemental frequencies relative to carbon) are based on those of dry biomass ($CH_{1.8}O_{0.5}N_{0.15}$), so $n^d_{C*_2} = 1$, $n^d_{H*_2} = 1.8$, $n^d_{O*_2} = 0.5$ and $n^d_{N*_2} = 0.15$ for $*_2 \in \{X, V, E, P\}$. The default water contents of food, structure, reserve and faeces are taxon-specific at phylum or class level (see function `get_d_V` of DEBtool Anonymous, 2019c) and are all equal $d_X = d_V = d_E = d_P$. The chemical indices of wet mass $n^w_{*1*_2}$ relate to that of dry mass $n^d_{*1*_2}$ for $*_1 \in \{H, O\}$ and $*_2 \in \{X, V, E, P\}$ is as follows. Let us call the number of H_2O molecules per C-atom x, so $n^w_{H*_2} = 2x + n^d_{H*_2}$ and $n^w_{O*_2} = x + n^d_{O*_2}$, while $n^w_{C*_2} = n^d_{C*_2}$ and $n^w_{N*_2} = n^d_{N*_2}$. The molecular weights of wet mass relates to that of dry mass as $w^w_{*_2} = w^d_{*_2} + 18x$, so $x = \frac{w^w_{*_2} - w^d_{*_2}}{18} = \frac{1 - d^d_{*_2}/d^w_{*_2}}{18}$, while $d^w_{*_2} \simeq 1$ g/cm^3. The molecular weight of dry mass relates to the chemical indices as $w^d_{*_2} = 12 + n_{H*_2} + 16n_{O*_2} + 14n_{N*_2}$ for $*_2 \in \{X, V, E, P\}$.

The chemical coefficients of the minerals are organised in a matrix $\boldsymbol{n}_M$, with chemical elements (C, H, O, N) in the rows and minerals (C, H, O, N) in the columns. That of the organics in matrix $\boldsymbol{n}_O$, with organics (X, V, $\mathrm{V}_{\dagger}$, E, $\mathrm{E}_{\dagger}$, P). Since we work in C-moles, the first row of $\boldsymbol{n}_O$ has elements 1 only.

The default values for the chemical potentials are set at $\mu_X = 525$ kJ, $\mu_V = 500$ kJ, $\mu_E = 550$ kJ, $\mu_P = 480$ kJ (see function `addchem` of DEBtool Anonymous, 2019c). Those of the minerals are zero, but for urea it is $\mu_N = 122$ kJ and for uric acid $\mu_N = 244/5$ kJ. We need them to evaluate the yield of heat on food and the yield of faeces on food.

Suppose that the population is in balanced growth condition and has a density of individuals (i.e. number per volume or surface area of environment) of $N = N_{0b} + N_{bi}$, where N_{0b} is the embryo density, N_{bi} the density of post-natals. The fraction of individuals that is embryo is

$\theta_{b0} = \frac{N_{b0}}{N} = \frac{\int_0^{a_b} \exp(-\dot{r}_N a) S(a)\, da}{\int_0^{\infty} \exp(-\dot{r}_N a) S(a)\, da}$. This directly follows from the stable age distribution, Eq. (2). The fraction of post-natals that is adult amounts to $\delta_{an} = \frac{\theta_{pi}}{\theta_{bp} + \theta_{pi}}$.

The mean structural length to the power i of post-natals is $\mathcal{L}_{bi}^i = \frac{\int_{a_b}^{\infty} L(a)^i \exp(-\dot{r}_N a) S(a)\, da}{\int_{a_b}^{\infty} \exp(-\dot{r}_N a) S(a)\, da}$, cf de Roos (2008).

The mean reproduction rate of adults is $\dot{\mathcal{R}} = \kappa_R \frac{[E_m]}{E_0} \left((1-\kappa) \frac{fg}{f+g} (\dot{v} \mathcal{L}_{pi}^2 + \dot{k}_M \mathcal{L}_{pi}^3) - \dot{k}_J E_H^p \right)$, where E_0 denotes the energy cost of an egg, $[E_m]$ the maximum reserve density, $\dot{k}_J$ the maturity maintenance rate coefficient, E_H^p the maturity at puberty, $\dot{v}$ the energy conductance, g the energy investment ratio, κ the allocation fraction to soma and κ_R the reproduction efficiency.

We now work out the yield coefficients for the organics, expressing them as ratios of individual-specific mass fluxes $\mathcal{J}$. The yield of food on food equals -1 by definition, $Y_{XX} = -1$; negative since food disappears, rather than appears. Population-level food consumption per unit of surface area or volume of environment amounts to $\dot{J}_X = f \{\dot{J}_{Xm}\} \mathcal{L}_{bi}^2$.

Population-level (living) structure production is $\dot{J}_V = [M_V] \left(S_b \delta_{an} \dot{\mathcal{R}} L_b^3 + \frac{\int_{a_b}^{\infty} \dot{r}(a) L(a)^3 \exp(-\dot{r}_N a) S(a)\, da}{\int_{a_b}^{\infty} \exp(-\dot{r}_N a) S(a)\, da} \right)$, where $\dot{r}$ is the specific growth rate of structure. So the yield of structure on food is $Y_{VX} = \frac{\dot{J}_V}{\dot{J}_X}$. Given the hazard rate $\dot{h}(a)$, the production of dead structure is $\dot{J}_V^{\dagger} = [M_V] \left((1-S_b) \delta_{an} \dot{\mathcal{R}} L_b^3 + \frac{\int_{a_b}^{\infty} \dot{h}(a) L(a)^3 \exp(-\dot{r}_N a) S(a)\, da}{\int_{a_b}^{\infty} \exp(-\dot{r}_N a) S(a)\, da} \right)$, so the yield of dead structure on food is $Y_{VX}^{\dagger} = \frac{\dot{J}_V^{\dagger}}{\dot{J}_X}$.

Likewise, reserve production at population level is $\dot{J}_E = \frac{f[E_m]}{\mu_E [M_V]} \dot{J}_V$ and that of dead reserve $\dot{J}_E^{\dagger} = \frac{f[E_m]}{\mu_E [M_V]} \dot{J}_V^{\dagger}$, so $Y_{EX} = \frac{\dot{J}_E}{\dot{J}_X}$ and $Y_{EX}^{\dagger} = \frac{\dot{J}_E^{\dagger}}{\dot{J}_X}$. The composition of the reproduction buffer is identical to that of reserve, which is why they are added, and it is empty till puberty, so $E_R(a) = 0$ for $a < a_p$. The population trait-pages of AmP assume for the s- and a-models the buffer handling rule of laying an egg as soon the buffer allows. Therefor the contribution of E_R in the yield coefficients is ignored.

The yield of faeces on food is $Y_{PX} = \kappa_P \frac{\mu_X}{\mu_P}$, where parameter κ_P is the fraction of food consumption, that is fixed in faeces.

The yield of heat on food (dimension energy per C-mol) amounts to $\mu_{TX} = \mu_X - (Y_{VX} + Y_{VX}^{\dagger}) \mu_V - (Y_{EX} + Y_{EX}^{\dagger}) \mu_E - Y_{PX} \mu_P - Y_{NX} \mu_N$. Notice that $\mu_N = 0$ in a combustion frame of reference if the N-waste is ammonia.

The yields for the minerals $\boldsymbol{Y}_M = (Y_{CX}, Y_{HX}, Y_{OX}, Y_{NX})$ follow from those for the organic ones $\boldsymbol{Y}_O = (Y_{XX}, Y_{VX}, Y_{VX}^{\dagger}, Y_{EX}, Y_{EX}^{\dagger}, Y_{PX})$ by conservation of chemical elements: $\boldsymbol{Y}_M = -\boldsymbol{n}_M^{-1} \boldsymbol{n}_O \boldsymbol{Y}_O$, cf (Kooijman, 2010b, Eq. (4.35)).

This completes the specification of the coefficients of the macro-chemical reaction equation.

Appendix B. Specific growth at maximum growth vs maximum specific growth of structure

The paper talks about the specific growth rate of structure at maximum growth. We here work out its relationship with a related quantity, the postnatal maximum specific growth of structure, for the standard DEB model, with zero surface-area related somatic maintenance and abundant food ($f = 1$).

Postnatal growth, i.e. change in structural volume, is given by (Kooijman, 2010b, Eq. (2.21))

$$\frac{d}{dt} L^3 = \dot{r} L^3 \quad \text{and specific growth rate of structure } \dot{r} = \dot{v} \frac{1/L - 1/L_m}{1+g} = \frac{\dot{k}_M (L_m/L - 1)}{1 + 1/g} \tag{B.1}$$

with $\dot{v}$ the energy conductance, $\dot{k}_M$ the somatic maintenance rate coefficient, g the energy investment ratio and $L_m = \frac{\dot{v}}{\dot{k}_M g}$ the maximum length. Alternatively, change in length is

$$\frac{d}{dt} L = \dot{r}_B (L_m - L) \quad \text{and von Bertalanffy growth rate } \dot{r}_B = \frac{\dot{k}_M/3}{1 + 1/g} = \frac{\dot{r}/3}{L_m/L - 1} \tag{B.2}$$

This change in length is known as the von Bertalannfy growth equation (Pütter, 1920). Growth is at maximum if $\frac{d}{dt} \dot{r} L^3 = 0$, which occurs at structural length $L = \frac{2}{3} L_m$, see (Kooijman, 2010b, page 312) and the specific growth rate at this length is $\dot{r}_m = \frac{\dot{k}_M / 2}{1 + 1/g}$. The implication is that the specific growth at maximum growth relates in a simple way to the von Bertalanffy growth rate: $\dot{r}_m = \frac{3}{2} \dot{r}_B$. As far as we know, this is a new interpretation of the von Bertalanffy growth rate.

The specific growth rate of structure only decreases after birth, making it maximum at birth, so at $L = L_b$ and has the value $\frac{\dot{k}_M (L_m / L_b - 1)}{1 + 1/g}$. So if $L_m > \frac{3}{2} L_b$, the maximum specific growth of structure exceeds the specific growth at maximum growth of structure, which is typically the case. The specific growth rate of structure at the start of embryo development is infinitely large, so we excluded the embryo stage here.

Appendix C. AmP Model specification

The notation follows the rules described in Kooijman (2020a). Add_my_Pet has 10 related DEB models, which as classified according to their acceleration behaviour: s-models with no acceleration, a-models with acceleration and h-models with acceleration and extra life stages. The entries follow the basic temperature correction (see below), unless parameters are specified for the extended version.

The environmental variables, temperature $T(t)$ and food density $X(t)$, can change in time t. All models are variations on the standard (std) model and all models deal with environmental variables in the same way:

Effect of temperature on any rate $\dot{k}$:

Basic: $\frac{\dot{k}(T)}{\dot{k}(T_{\text{ref}})} = \exp\left(\frac{T_A}{T_{\text{ref}}} - \frac{T_A}{T} \right)$

Extended: $\frac{\dot{k}(T)}{\dot{k}(T_{\mathrm{ref}})} = \exp\left(\frac{T_A}{T_{\mathrm{ref}}} - \frac{T_A}{T}\right) \frac{1 + \exp\left(\frac{T_{AL}}{T_{\mathrm{ref}}} - \frac{T_{AL}}{T_L}\right)_+ + \exp\left(\frac{T_{AH}}{T_H} - \frac{T_{AH}}{T_{\mathrm{ref}}}\right)_+}{1 + \exp\left(\frac{T_{AL}}{T} - \frac{T_{AL}}{T_L}\right)_+ + \exp\left(\frac{T_{AH}}{T_H} - \frac{T_{AH}}{T}\right)_+}$

Effect of food on assimilation: if $E_H < E_H^b$, $\dot{p}_X = 0$, else $\dot{p}_X = f\{\dot{p}_{Xm}\}L^2$ with $f = \frac{X}{K+X}$ and $K = \frac{\{\dot{J}_{Xm}\}}{\{\dot{F}_m\}}$ and $\{\dot{p}_{Xm}\} = s_M\{\dot{p}_{Am}\}/\kappa_X$ with acceleration factor $s_M = \min(L, L_j)/L_s$

C1. s-models

s-models assume isomorphy throughout the full life cycle, so no acceleration ($L_j = L_s = L_b$ and $s_M = 1$).

C1.1. std model

The std-model follows from the assumptions as listed in (Kooijman, 2010b, Table 2.4).
Within the family of DEB models, the std-model can be seen as a canonical form.
Main characteristics:

- 1 type of food X, 1 type of structure V, 1 type of reserve E, 1 type of feces P
- 4 minerals (carbon dioxide C, water H, dioxygen O, N-waste N); O is not limiting
- 3 life stages (embryo, juvenile, adult) triggered by maturity thresholds
  - birth is defined as start of assimilation via food uptake
  - puberty as end of maturation and start of allocation to reproduction
- If mobilisation is not fast enough to cover maturity and/or somatic maintenance, rejuvenation and/or some shrinking can occur, but only after use of the reproduction buffer
- The reproduction buffer is continuously converted to a spawning buffer, which is instantaneously converted to exported eggs, if the spawning buffer exceeds a density threshold

Parameters:

Temperature: T_A, T_L, T_H, T_{AL}, T_{AH}
Hazard: $\ddot{h}_a$, s_G, δ_L, $\dot{h}_J$, $\dot{h}_0$, $\dot{h}_0^e$
Life stage: E_H^b, E_H^p
Core: $\{\dot{F}_m\}$, $\{\dot{p}_{Am}\}$, $[\dot{p}_M]$, $\{\dot{p}_T\}$, $\dot{k}_J$, $\dot{k}_J'$, $\dot{v}$, $[E_G]$, κ, κ_X, κ_P, κ_R, $[E_R^s]$
Chemical: $[M_V]$, $\boldsymbol{d}_O = (d_X \;\; d_V \;\; d_E \;\; d_P)$, $\boldsymbol{\mu}_O = (\overline{\mu}_X \;\; \overline{\mu}_V \;\; \overline{\mu}_E \;\; \overline{\mu}_P)$, $\boldsymbol{n}_M$, $\boldsymbol{n}_O^d$,
where the chemical coefficients for minerals and (dry) organic compounds are

$$\boldsymbol{n}_M = \begin{pmatrix} 1 & 0 & 0 & n_{CN} \\ 0 & 2 & 0 & n_{HN} \\ 2 & 1 & 2 & n_{ON} \\ 0 & 0 & 0 & n_{NN} \end{pmatrix} \text{ and } \boldsymbol{n}_O^d = \begin{pmatrix} 1 & 1 & 1 & 1 \\ n_{HX}^d & n_{HV}^d & n_{HE}^d & n_{HP}^d \\ n_{OX}^d & n_{OV}^d & n_{OE}^d & n_{OP}^d \\ n_{NX}^d & n_{NV}^d & n_{NE}^d & n_{NP}^d \end{pmatrix}.$$

If the N-waste is ammonia, we have $n_{CN} = 0$, $n_{HN} = 3$, $n_{ON} = 0$, $n_{NN} = 1$.

Help quantities (for the specification of changes in state):

wet/dry mass: The chemical coefficients of wet organic mass n_{*1*2}^w relate to that of dry mass n_{*1*2}^d for $*_1 \in \{H, O\}$ and $*_2 \in \{X, V, E, P\}$ as $n_{H*_2}^w = 2x_{*_2} + n_{H*_2}^d$ and $n_{O*_2}^w = x_{*_2} + n_{O*_2}^d$, while $n_{C*_2}^w = n_{C*_2}^d$ and $n_{N*_2}^w = n_{N*_2}^d$, where $x_{*_2} = \frac{1 - d_{*_2}^d / d_{*_2}^w}{18}$, while $d_{*_2}^w \simeq 1$ g/cm^3.

mass fluxes: $\dot{\boldsymbol{J}}_O = (\dot{J}_X \;\; \dot{J}_V \;\; (\dot{J}_E + \dot{J}_{E_R}) \;\; \dot{J}_P)$ relate to energy fluxes $\dot{\boldsymbol{p}} = (\dot{p}_A \;\; \dot{p}_D \;\; \dot{p}_G)$, as $\dot{\boldsymbol{J}}_O = \boldsymbol{\eta}_O \dot{\boldsymbol{p}}$ with $\boldsymbol{\eta}_O = \begin{pmatrix} -\frac{1}{\kappa_X \overline{\mu}_X} & 0 & 0 \\ 0 & 0 & \frac{\kappa_G}{\overline{\mu}_V} \\ \frac{1}{\overline{\mu}_E} & -\frac{1}{\overline{\mu}_E} & -\frac{1}{\overline{\mu}_E} \\ \frac{\kappa_P}{\kappa_X \overline{\mu}_P} & 0 & 0 \end{pmatrix}$ and $\kappa_G = \overline{\mu}_V \frac{[M_V]}{[E_G]}$

assimilation: $\dot{p}_A = \kappa_X \dot{p}_X$
somatic maintenance: $\dot{p}_S = [\dot{p}_S]L^3$. If $E_H < E_H^b$, $[\dot{p}_S] = [\dot{p}_M]$, else $[\dot{p}_S] = [\dot{p}_M] + \{\dot{p}_T\}/L$
maturity maintenance: if $(1-\kappa)\dot{p}_C > \dot{k}_J E_H$ (no rejuvenation), $\dot{p}_J = \dot{k}_J E_H$, else $\dot{p}_J = \dot{k}_J' E_H$
mobilization: $\dot{p}_C = E(\dot{v}/L - \dot{r})$. If $[E] \geq \frac{[\dot{p}_S]L}{\dot{v}\kappa}$ (no shrinking), $\dot{r} = \frac{[E]\dot{v}/L - [\dot{p}_S]/\kappa}{[E] + [E_G]/\kappa}$, else if $E_R > 0$, $\dot{r} = 0$, or if $E_R \leq 0$, $\dot{r} = \frac{[E]\dot{v}/L - [\dot{p}_S]/\kappa}{[E] + [E_G]\kappa_G/\kappa}$ (shrinking)
growth: $\dot{p}_G = \kappa\dot{p}_C - \dot{p}_S$, but if $\kappa\dot{p}_C < \dot{p}_S$ and $E_R > 0$: $\dot{p}_G = 0$
maturation/reproduction: $\dot{p}_R = (1-\kappa)\dot{p}_C - \dot{p}_J$, but if $(1-\kappa)\dot{p}_C < \dot{p}_J$ and $E_R > 0$: $\dot{p}_R = 0$
dissipation: if $E_H < E_H^p$, $\dot{p}_D = \dot{p}_S + \dot{p}_J + \dot{p}_R$, else $\dot{p}_D = \dot{p}_S + \dot{p}_J + (1-\kappa_R)\dot{p}_R$

Initial states: $L(0) = 0$, $E_H(0) = 0$, $E_R(0) = 0$, $\ddot{q}(0) = 0$, $\dot{h}_A(0) = 0$ and $E(0) = E_0$ such that $[E](a_b)$ equals that of mother at egg production
Changes in state :

structure: $\frac{d}{dt}L = L\dot{r}/3$. So, initial change is $\frac{d}{dt}L(0) = \dot{v}/3$

reserve: If $E_H < E_H^b$ (embryo), $\frac{d}{dt}[E] = -[E]\dot{v}/L$, else $\frac{d}{dt}[E] = (\{\dot{p}_{Am}\}f - [E]\dot{v})/L$

maturity: If $E_H < E_H^p$ (embryo or juvenile), $\frac{d}{dt}E_H = \dot{p}_R$, else $\frac{d}{dt}E_H = 0$. However, if $\dot{p}_J < 0$ and $E_R = 0$ (rejuvenation), $\frac{d}{dt}E_H = \dot{p}_J'$ with $\dot{p}_J' = \min(0, \dot{p}_J \dot{k}_J'/\dot{k}_J)$

buffer: If $E_H = E_H^p$ (adult), $\frac{d}{dt}E_R = \dot{p}_R - \dot{p}_J' - \dot{p}_G'$, else $(E_H < E_H^p)$ $\frac{d}{dt}E_R = 0$. If adult and $E_R > 0$, $\dot{p}_G' = \max(0, [\dot{p}_S]L^3 - \kappa\dot{p}_C)$, else $(E_R \leq 0)$ $\dot{p}_J' = 0$ and $\dot{p}_G' = 0$. The buffer is partitioned as $E_R = E_R^0 + E_R^1$, where E_R^0 converts, for positive E_R^0, to E_R^1 at rate $\dot{p}_R^{\max} = \frac{1-\kappa}{\kappa}L^3\frac{[E_G]\dot{v}/L + [\dot{p}_S]}{1+g} - \dot{p}_J$ and $g = \frac{[E_G]\dot{v}}{\kappa\{\dot{p}_{Am}\}}$.

hazard: $\dot{h} = \dot{h}_A + \dot{h}_X + \dot{h}_B + \dot{h}_P$

- aging: $\frac{d}{dt}\ddot{q} = (\ddot{q}\frac{L^3}{L_m^3}s_G + \ddot{h}_a)e(\frac{\dot{v}}{L} - \dot{r}) - \dot{r}\ddot{q}$; $\quad \frac{d}{dt}\dot{h}_A = \ddot{q} - \dot{r}\dot{h}_A$
- starving (food): If $E_H < E_H^b$, $\dot{h}_X = 0$, else if $\dot{p}_C < \frac{\dot{k}_J E_H}{1-\kappa}$, $\dot{h}_X = \dot{h}_J(1 - \frac{\dot{p}_C(1-\kappa)}{\dot{k}_J E_H})$.
  Let L_0 be the length at which $\dot{r} = 0$ for the last time.
  If $L = \delta_L L_0$, $h_X\, dt = \infty$ (instant death due to shrinking)
- accidental (background): If $E_H < E_H^b$, $\dot{h}_B = \dot{h}_B^{0b}$, else $\dot{h}_B = \dot{h}_B^{bi}$; both constant
- thinning (predation): If $E_H \geq E_H^b$, $\dot{h}_P = \frac{2}{3}\dot{r}$, else $\dot{h}_P = 0$

Input/output fluxes:

food: $\dot{J}_X = \frac{\dot{p}_A}{\kappa_X \overline{\mu}_X}$

feces: $\dot{J}_P = \frac{\kappa_P \dot{p}_A}{\kappa_X \overline{\mu}_P}$

eggs: If $E_R^1 = [E_R^s]L^3$: $\dot{R}\, dt = \kappa_R[E_R^s]L^3/E_0$ eggs are produced and E_R^1 is set to 0

minerals: $\dot{\boldsymbol{J}}_{\mathcal{M}} = -\boldsymbol{n}_{\mathcal{M}}^{-1}\boldsymbol{n}_O^w\dot{\boldsymbol{J}}_O$, where $\dot{\boldsymbol{J}}_{\mathcal{M}} = (\dot{J}_C \;\; \dot{J}_H \;\; \dot{J}_O \;\; \dot{J}_N)$

heat: $\dot{p}_{T+} = -\overline{\boldsymbol{\mu}}_O^T\dot{\boldsymbol{J}}_O$

death: at death, $[M_V]L^3$ moles of structure and $(E + E_R)/\overline{\mu}_E$ moles of reserve become available in the environment

C1.2. stf-model

Like the std-model but with

- fetal development (rather than egg development, see also the stx-model)

Budding, as found in cnidarians and salps has, metabolically, similarities with fetal propagation: no assimilation by buds during development. This type of fetal development is found in e.g. some cartilaginous and ray-finned fish, Peripatus.

The deviation from the standard model amounts for the fetus, which has $E_H < E_H^b$, to $E(0) = 0$ and $\frac{d}{dt}[E] = (\{\dot{p}_{Am}\}f - [E]\dot{v})/L$, where f equals the value of the mother. For the mother, the deviation amounts to $\frac{d}{dt}E_R = \dot{p}_R - n\{\dot{p}_{Am}\}fL_e^2$, where L_e is the structural length of the fetus, n the number of fetuses, such that $\dot{p}_R a_b = nf\{\dot{p}_{Am}\}\int_0^{a_b} L_e^2(t)\, dt$. The effect is that $E_R = 0$ at the end of the gestation period.

C1.3. stx-model

Like the stf-model but with

- fetal development (rather than egg development) that first starts with a preparation stage and then sparks off at a time, t_0, that is an extra parameter
- a baby stage (for mammals) just after birth, ended by weaning, where the juvenile switches from feeding on milk to solid food at maturity level E_H^x. Weaning is between birth and puberty, so $E_H^b \leq E_H^x \leq E_H p$.

In its simplest form, it is a two parameter extension of std-model at abundant food. Food quality and up-regulation of assimilation can involve more parameters. This life history is found in placentalia. Milk production is from up-regulated feeding/assimilation.

C1.4. ssj-model

Like the std-model but with

- a non-feeding stage between events s and j during the juvenile stage that is initiated at a particular maturity level, E_H^s and lasts a particular time, t_{sj}. Substantial metabolically controlled shrinking occurs during this period, with specific rate $\dot{k}_E$, faster than can be explained by starvation.

It is a three parameter extension of the std-model. Event s is in this model not the start of acceleration, but that of shrinking. This life history is found in Elopiformes, Albuliformes, Notacanthiformes, Anguilliformes, Ophidiiformes, some Anura and Echinodermata. The comments (Kooijman, 2010a, Section 7.8.3) give more background.

Given $V = V_s$, $E = E_s$, $E_H = E_H^s$ at time t, $V = \delta_{sj}V_s$, $E = \delta_{sj}E_s$ and $E_H = \delta_{sj}E_H^s$ at time $t + t_{sj}$, with $\delta_{sj} = \exp(-\dot{k}_E\delta_{sj})$, while $\dot{p}_X = 0$ for $t \in (t, t + t_{sj})$.

C1.5. sbp-model

Like the std model but with

- growth ceases at puberty, meaning that the κ-rule is not operational in adults.

It has the same parameters as the std-model, and is similar to the abp-model, which differs by acceleration. This life history is found in Calanus, while other copepods accelerate.

At puberty, growth ceases. so $\dot{p}_G = 0$, and the κ-rule no longer applies. Mobilisation after puberty is $\dot{p}_C = \dot{v}E/L_p$, and allocation to reproduction is $\dot{p}_R = \dot{p}_C - \dot{p}_M - \dot{p}_J$, with $\dot{p}_J = \dot{k}_J E_H^p$.

C2. a-models

a-models also assume isomorphy, but during part of the life cycle metabolism accelerates following the rules for V1-morphy. During this period, the acceleration factor increases proportional to length from 1 till $s_M = L_j/L_s$.

C2.1. abj-model

The DEB model with type M acceleration is like std-model, but

- acceleration between birth b and metamorphosis j ($L_s = L_b$)
- before and after acceleration: isomorphy

Metamorphosis is before puberty and occurs at maturity E_H^j, so $E_H^b \leq E_H^j \leq E_H p$, which might or might not correspond with changes in morphology. Type M acceleration has never been found in cartilaginous fish, amphibians, reptiles, birds or mammals, and typically occurs in taxa with larval stages.

The abj-model is a one-parameter extension of std-model and reduces to the std-model for $E_H^j = E_H^b$. During metabolic acceleration, $\{\dot{p}_{Am}\} = \{\dot{p}_{Am}^b\}L/L_b$ and $\dot{v} = \dot{v}^b L/L_b$, where $\{\dot{p}_{Am}^b\}$ and $\dot{v}^b$ refer to the values at birth. At j, acceleration ceases: $\{\dot{p}_{Am}\} = \{\dot{p}_{Am}^b\}s_M$ and $\dot{v} = \dot{v}^b s_M$, with acceleration factor $s_M = L_j/L_b$.

C2.2. asj-model

The DEB model with delayed type M acceleration is like abj-model, but

- start of acceleration is delayed till maturity level E_H^s and lasts till metamorphosis at maturity level E_H^j
- Before and after acceleration: isomorphy

Metamorphosis is still before puberty, so $E_H^b \leq E_H^s \leq E_H^j \leq E_H p$ and the acceleration factor is $s_M = L_j/L_s$. This model is a one-parameter extension of the abj-model and reduces to the std-model for $E_H^b = E_H^s = E_H^j$. This life history is found in Mnemiopsis, Crassostrea and Aplysia. Further improvement of data might require a change from abj- to asj-models for quite a few species.

C2.3. abp-model

The DEB model with type M acceleration is like model-abj, but

- acceleration between birth and puberty ($L_s = L_b$)
- before acceleration: isomorphy
- after acceleration: no growth

Metamorphosis can occur before puberty and occurs at maturity E_H^j, but only affects morphology, not metabolism. This model has the same number of parameters as the std-model. The acceleration factor is $s_M = L_p/L_b$. It is similar to the sbp-model, which has no acceleration. It applies to copepods, may be also to ostracods, spiders and scorpions.

At puberty, growth ceases, so $\dot{p}_G = 0$. Mobilisation after puberty is $\dot{p}_C = s_M \dot{v}E/L_p = \dot{v}E/L_b$, and allocation to reproduction is $\dot{p}_R = \dot{p}_C - \dot{p}_M - \dot{p}_J$, with $\dot{p}_J = \dot{k}_J E_H^p$.

C3. h-models

h-models also assume isomorphy, but during part of the life cycle metabolism accelerates following the rules for V1-morphy

C3.1. hep-model

The DEB for ephemeropterans, odonata and possibly other insect groups. Its characteristics are

- morphological life stages: egg, larva, (sub)imago; functional stages: embryo, juvenile, adult, imago
- the embryo still behaves like the std-model
- acceleration starts at birth and ends at puberty ($L_s = L_b$)
- puberty occurs during the larval stage
- emergence of the imago occurs when reproduction buffer density, $E_R/L^3 = [E_R^j]$, hits a threshold
- the (sub)imago does not grow or allocate to reproduction. It mobilizes reserve to match constant (somatic plus maturity) maintenance

The model is discussed in the comments (Kooijman, 2010a, Section 7.8). The difference with the abp-model is that growth continues at puberty, ceasing of growth uses on another trigger and imago's don't allocate to reproduction.

Between p and j, allocation to reproduction is $\dot{p}_R = (1-\kappa)\dot{p}_C - \dot{p}_J$. After j, mobilisation is $\dot{p}_C = \dot{p}_M + \dot{p}_J$, allocation to reproduction is $\dot{p}_R = 0$.

C3.2. hex-model

The DEB model for holometabolic insects (and some other hexapods). Its characteristics are

- morphological life stages: egg, larva, (pupa), imago; functional stages: embryo, adult, (pupa), imago
- the embryo still behaves like the std-model
- the larval stage accelerates (V1-morph) and behaves as adult, i.e. no maturation ($L_b = L_s = L_p$), allocation to reproduction and $E_H^b = E_H^p$.
- pupation occurs when reproduction buffer density hits a threshold, $E_R/L^3 = [E_R^j]$
- pupa behaves like an isomorphic embryo of the std-model, emergence occurs at $E_H = E_H^e$ Larval structure rapidly transforms to pupal reserve just after start of pupation, and sets $E_H = 0$ at j.
- the reproduction buffer remains unchanged during the pupal stage
- the imago does not grow or allocate to reproduction. Imago's reserve mobilisation matched somatic plus maturity maintenance $\dot{p}_C = \dot{p}_M + \dot{p}_J$.

Hemi-metabolic insects skip the pupal stage, don't convert larval structure to reserve. Imago structure equals larval structure when reproduction buffer density hits a threshold. The model is discussed in the comments (Kooijman, 2010a, Section 7.8).

For $\dot{k}_E = \dot{v}/L_b$, reserve mobilisation prior to pupation (i.e. during acceleration) is $\dot{p}_C = E(\dot{k}_E - \dot{r})$ with $\dot{r} = \frac{\kappa[E]\dot{k}_E - [\dot{p}_M]}{\kappa[E] + [E_G]} = g\dot{k}_M \frac{e/l_b - 1}{e+g}$. The larva allocates to reproduction as $\dot{p}_R = (1-\kappa)\dot{p}_C - \dot{p}_J$, with $\dot{p}_J = \dot{k}_J E_H^p$. $[E_R]$ has a maximum at $[E_R^m] = [E_R^{\text{ref}}] f \frac{1-l_b}{f-l_b}$ with $[E_R^{\text{ref}}] = (1-\kappa)[E_m]\frac{g+l_b}{1-l_b}$, so pupation occurs when $[E_R] = s_j[E_R^{\text{ref}}]$, with $s_j = [E_R^j]/[E_R^{\text{ref}}]$.

Reserve mobilisation of the imago is $\dot{p}_C = \dot{p}_M^e + \dot{p}_J^e$, where $\dot{p}_M^e = [\dot{p}_M]L_e^3$ and $\dot{p}_J^e = \dot{k}_J E_H^e$.

Supplementary material

Supplementary material associated with this article can be found, in the online version, at 10.1016/j.ecolmodel.2020.109055.

References

Anonymous, 2019a. AmP collection. https://www.bio.vu.nl/thb/deb/deblab/add_my_pet/.

Anonymous, 2019b. Software package AmPtool. http://www.github.com/add-my-pet/AmPtool/.

Anonymous, 2019c. Software package DEBtool. http://www.github.com/add-my-pet/DEBtool_M/.

Augustine, S., Gagnaire, B., Adam, C., Kooijman, S.A.L.M., 2011. Developmental energetics of zebrafish, Danio rerio. Comp. Physiol. Biochem. A 159, 275–283.

Augustine, S., Lika, K., Kooijman, S.A.L.M., 2019. Altricial-precocial spectra in animal kingdom. J. Sea Res 143, 27–34.

Augustine, S., Lika, K., Kooijman, S.A.L.M., 2019. Why big-bodied animal species cannot evolve a waste-to-hurry strategy. J. Sea Res. 143, 18–26.

Brown, J.H., Allen, A.P., Gillooly, J.F., 2007. The metabolic theory of ecology and the role of body size in marine and freshwater ecosystems. In: Hildrew, A.G., Raffaelli, D.G., Edmonds-Brown, R. (Eds.), Body size: The structure and function of aquatic ecosystems. British Ecologycal society.

Gompertz, B., 1825. On the nature of the function expressive of the law of mortality, and on a new method of determining the value of life contingencies. Phil. Trans. R. Soc. Lond. B Biol. Sci. 27, 513–585.

Huxley, J.S., 1932. Problems of Relative Growth. Methuen, London.

Jusup, M., Sousa, T., Domingos, T., Labinac, V., Marn, N., Wang, Z., Klanjscek, T., 2017. Physics of metabolic organization. Phys. Life Rev. 20, 1–39.

Kleiber, M., 1932. Body size and metabolism. Hilgardia 6, 315–353.

Kooi, B.W., Kooijman, S.A.L.M., 1994. Existence and stability of microbial prey-predator systems. J. Theor. Biol. 170, 75–85.

Kooijman, S.A.L.M., 1986. Energy budgets can explain body size relations. J. Theor. Biol. 121, 269–282.

Kooijman, S.A.L.M., 1986. Population Dynamics on the Basis of Budgets. Springer-Verlag, Berlin. The dynamics of physiologically structured populations, Springer Lecture Notes in Biomathematics, pages 266–297

Kooijman, S.A.L.M., 1992. Biomass Conversion at Population Level. Chapman & Hall. Individual based models; an approach to populations and communities, pages 338–358

Kooijman, S.A.L.M., 2001. Quantitative aspects of metabolic organization; a discussion of concepts. Phil. Trans. R. Soc. B 356, 331–349.

Kooijman, S. A. L. M., 2010a. Comments on the DEB book, Kooijman. https://www.bio.vu.nl/thb/research/bib/Kooy2010_c.pdf 2020.

Kooijman, S.A.L.M., 2010b. Dynamic Energy Budget Theory for Metabolic organisation. Cambridge University Press.

Kooijman, S.A.L.M., 2012. Energy Budgets. University of California Press. Sourcebook in Theoretical Ecology, pages 249–258

Kooijman, S.A.L.M., 2013. Waste to hurry: dynamic energy budgets explain the need of wasting to fully exploit blooming resources. Oikos 122, 348–357.

Kooijman, S.A.L.M., 2014. Metabolic acceleration in animal ontogeny: an evolutionary perspective. J. Sea Res. 94, 128–137.

Kooijman, S. A. L. M., 2020a. https://www.bio.vu.nl/thb/research/bib/Kooy2010_n.pdf. DEB notation.

Kooijman, S.A.L.M., 2020b. The standard dynamic energy budget model has no plausible alternatives. Ecol. Mod this volume:submitted.

Kooijman, S.A.L.M., Lika, K., 2014. Comparative energetics of the 5 fish classes on the basis of dynamic energy budgets. J. Sea Res. 94, 19–28.

Kooijman, S.A.L.M., Lika, K., 2014. Resource allocation to reproduction in animals. Biol. Rev. 89, 849–859.

Kooijman, S.A.L.M., Metz, J.A.J., 1984. On the dynamics of chemically stressed populations; the deduction of population consequences from effects on individuals. Ecotox. Environ. Saf. 8, 254–274.

Kooijman, S.A.L.M., Pecquerie, L., Augustine, S., Jusup, M., 2011. Scenarios for acceleration in fish development and the role of metamorphosis. J. Sea Res. 66, 419–423.

Kot, M., 2001. Elements of Mathematical Ecology. Cambridge University Press, Cambridge.

Ledder, G., 2014. The basic dynamic energy budget model and some implications. Lett. Biomath. 1, 221–233.

van Leeuwen, I.M.M., Kelpin, F.D.L., Kooijman, S.A.L.M., 2002. A mathematical model that accounts for the effects of caloric restriction on body weight and longevity. Biogerontology 3, 373–381.

Lika, K., Augustine, S., Kooijman, S.A.L.M., 2019. Body size as emergent property of metabolism. J. Sea Res. 143, 8–17.

Lika, K., Augustine, S., Pecquerie, L., Kooijman, S.A.L.M., 2014. The bijection from data to parameter space with the standard deb model quantifies the supply-demand spectrum. J. Theor. Biol. 354, 35–47.

Marques, G.M., Augustine S., S.A., Lika, K., Pecquerie, L., Domingos, T., Kooijman, L.M., 2018. The AmP project: comparing species on the basis of dynamic energy budget parameters. PLoS Comput. Biol. 14 (5), E1006100.

Marques, G.M., Lika, K., Augustine, S., Pecquerie, L., Kooijman, S.A.L.M., 2019. Fitting multiple models to multiple data sets. J. Sea Res. 143, 48–56.

van der Meer, J., 2006. An introduction to dynamic energy budget (DEB) models with special emphasis on parameter estimation. J. Sea Res. 56, 85–102.

van der Meer, J., 2016. A paradox in individual-based models of populations. Conserv. Physiol. 1 (1).

Muller, E.R., Lika, K., Nisbet, R.M., Schultz, I.R., Casas, J., Gergs, A., Murphy, C., Nacci, D., Watanabe, K.H., 2019. Regulation of reproductive processes with dynamic energy budgets. Func. Ecol. 33, 819–832.

Pielou, E.C., 1969. An Introduction to Mathematical Ecology. Wiley, New york.

Pütter, A., 1920. Studien über physiologische Ähnlichkeit. VI Wachstumsähnlichkeiten. Arch. Gesamte Physiol. Mench. Tiere 180, 298–340.

Ricklefs, R.E., Scheuerlein, A., 2002. Biological implications of the Weibull and Gompertz models of aging. J. Gerontology 57A, B69–B76.

de Roos, A.M., 1997. A Gentle Introduction to Physiologically Structured Population Models. Chapman & Hall, New York. Structured-Population models in marine, terrestrial, and freshwater systems, 119–204

de Roos, A.M., 2008. Demographic analysis of continuous-time life-history models. Ecol. Lett. 11, 1–15.

Sara, G., Rinaldi, A., Montalto, V., 2014. Thinking beyond organism energy use: a trait-based bioenergetic mechanistic approach for predictions of life history traits in marine organisms. Mar. Ecol. 35, 506–515.

Savage, V.M., Gillooly, J.F., Brown, J.H., West, G.B., Charnov, E.L., 2004. Effects of body size and temperature on population growth. Am. Nat. 163, 429–441.
Schmidt, J., 1921. New studies of sun-fishes made during the “dana” expedition. Nature 107, 76–79.
Sousa, T., Domingos, T., Kooijman, S.A.L.M., 2008. From empirical patterns to theory: a formal metabolic theory of life. Phil. Trans. R. Soc. B 363 (1502), 2453–2464.
Sousa, T., Domingos, T., Poggiale, J.-C., Kooijman, S.A.L.M., 2010. Dynamic energy budget theory restores coherence in biology. Phil. Trans. R. Soc. B 365 (1557), 3413–3428.
Sousa, T., Mota, R., Domingos, T., Kooijman, S.A.L.M., 2006. The thermodynamics of organisms in the context of dynamic energy budget theory. Phys. Rev. E 74 (51901), 1–15.
Weibull, W., 1951. A statistical distribution of wide applicability. J. Appl. Mech. 18, 293–297.